Programmable, very low noise current source

G. Scandurra, G. Cannatà, G. Giusi, and C. Ciofi
Dipartimento di Ingegneria Elettronica, Chimica e Ingegneria Industriale, University of Messina, Messina 98166, Italy

(Received 27 August 2014; accepted 24 November 2014; published online 10 December 2014)

We propose a new approach for the realization of very low noise programmable current sources mainly intended for application in the field of low frequency noise measurements. The design is based on a low noise Junction Field Effect Transistor (JFET) acting as a high impedance current source and programmability is obtained by resorting to a low noise, programmable floating voltage source that allows to set the sourced current at the desired value. The floating voltage source is obtained by exploiting the properties of a standard photovoltaic MOSFET driver. Proper filtering and a control network employing super-capacitors allow to reduce the low frequency output noise to that due to the low noise JFET down to frequencies as low as 100 mHz while allowing, at the same time, to set the desired current by means of a standard DA converter with an accuracy better than 1%. A prototype of the system capable of supplying currents from a few hundreds of μA up to a few mA demonstrates the effectiveness of the approach we propose. When delivering a DC current of about 2 mA, the power spectral density of the current fluctuations at the output is found to be less than 25 pA/$\sqrt{\text{Hz}}$ at 100 mHz and less than 6 pA/$\sqrt{\text{Hz}}$ for $f > 1$ Hz, resulting in an RMS noise in the bandwidth from 0.1 to 10 Hz of less than 14 pA. © *2014 AIP Publishing LLC*. [http://dx.doi.org/10.1063/1.4903355]

I. INTRODUCTION

It has long been recognized that Low Frequency Noise Measurements (LFNM) can be a very sensitive tool for the investigation of the quality and reliability of electron devices.[1] In order to reach the highest sensitivity, however, care must be taken to minimize the noise contribution coming from the instrumentation employed for biasing the Device Under Test (DUT) and for amplifying the noise signal we are interested in.[2] At frequencies as low as a few Hz and below, it is the flicker noise introduced by the instrumentation that sets the background noise of the system. The equivalent input noise of the amplifier used for raising the level of the noise produced by the DUT sets the ultimate limit to the sensitivity that can be obtained only in the case in which the contribution to the background noise coming from the DUT bias network can be neglected. To insure this last condition, it is common practice to employ high capacity batteries and excess noise free resistors for realizing the biasing networks. In particular, a series of batteries for obtaining a sufficiently large voltage together with a sufficiently large series resistance can behave as a low noise current source for biasing a DUT in voltage noise measurements. While effective in most cases, this approach has several drawbacks: large volume occupied by batteries, need for frequent recharge, low accuracy and stability due to the change of the supplied voltage with charge state and temperature. Programmability can be obtained by employing relays for switching a network of resistances in such a way as to obtain different values of series resistances and, hence, different currents.[3] In other cases, a programmable solid state voltage source with a sufficiently large series resistance can be used to set the bias current through a sample with high resolution.[4] While effective in some cases, the abovementioned approaches can seldom provide the very high internal impedance that would be desirable for a current source. A very high output resistance insures that the current does not change appreciably when changing the load and can be valuable in applications such as noise measurement on unpackaged devices where the availability of a high output impedance current source together with a proper measurement configuration allows the rejection of the large amount of low frequency noise that generates at the contacts between the sample pads and the probe tips.[5] On the other hand, small size would be desirable for the integration of the current source as part of compact measurement systems.[6] Low noise current sources based on solid state devices with a very high equivalent output impedance can indeed be built by employing discrete low noise Junction Field Effect Transistors (JFETs) in a configuration such as the one reported in Fig. 1.[7] The DC voltage V_B is used together with the excess noise free resistor R_S to set the sourced current I_{OUT} according to the following relationship:

$$I_{OUT} = \frac{V_B - V_{GS}}{R_S}. \tag{1}$$

With V_B in the order of a few volts and by employing very low pinch off voltages JFETs, the dependence of I_{OUT} on the actual V_{GS} of the particular JFET being used can be made reasonably small. The power spectrum S_{IOUT} of the current noise sourced to the load can be calculated as follows:[8]

$$S_{IOUT} = \left(\frac{g_m R_S}{1 + g_m R_S}\right)^2 \frac{S_{VB} + S_j + 4kTR_S}{R_S^2}, \tag{2}$$

where g_m is the transconductance of the JFET, k is the Boltzmann constant, T the absolute temperature, S_{VB} and S_j are the power spectra of the voltage fluctuations e_{VB} of the source V_B and of the equivalent input noise source e_j of the JFET, respectively, and $4kTR_S$ is the power spectral density of the thermal noise source e_{RS} associated to the resistance R_S.

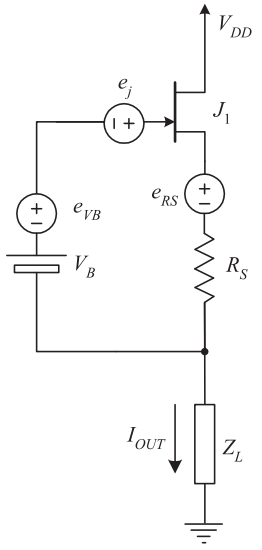

FIG. 1. A simple low noise current source. In its simplest realization, the voltage source V_B can be a battery.

The effect of the input current noise source at the gate of the JFET has not been included as its effect is generally negligible with respect to the other sources of noise. An obvious choice for implementing V_B is that of resorting to a battery that, since it does not supply a significant current during operation, behaves as a very low noise voltage source.[9] If one is willing to accept the significant dispersion in the sourced current that results from the dispersion in JFET characteristics, the voltage V_B can be avoided ($V_B = 0$) and proper trimming on R_S can be used for adjusting the current to the desired value. Indeed, by using a set of circuits such as the one in Fig. 1, each of which supplying a different current value (different values of R_S), and a switching and combining circuit, a programmable low noise current source has been proposed.[10]

There is, however, a significant advantage, from the point of view of the supplied current noise, in providing for a large value for V_B. This can be quite easily understood from Eqs. (1) and (2). The same supplied current can be obtained with the same V_{GS} (resulting in the same transconductance g_m) with different combinations of V_B and R_S. Clearly, for higher values of V_B, we need higher values of R_S resulting in lower noise levels as it is apparent from Eq. (2). Moreover, should we be able to design a programmable low noise voltage source to be used for V_B, we could clearly obtain a programmable low noise current source. While very low noise programmable voltage sources have been realized,[11,12] they cannot be directly used for V_B, since we need a floating low noise voltage source and this is not easily obtained, unless one is willing to employ two sets of battery packs floating with respect to each other[13] with the obvious drawback of larger volume, circuit complication and large parasitic effects that may easily lead to circuit instability and/or increased influence from external interferences.

The fact that the source V_B at steady state need only to supply a very low current (it actually needs to be capable of sinking the leakage current from the JFET gate that is in the order, at most, of a few pA), suggests the possibility of exploring miniaturized photovoltaic cells for generating a programmable voltage controlled by the light power emitted by a LED. Conventional optocouplers such as the 4N25 may act, under proper biasing, as controlled floating voltage sources and they have been successfully used in a few cases for easing offset correction.[14,15] The voltage that can be obtained at the output of this system, where one of the junctions of the output phototransistor acts as a tiny photoelectric source, is clearly limited to a fraction of 1 V and therefore a few tens of cells would be required for reaching voltages in the order of a few volts. Moreover, the current driving capability of such a source would be limited to a few μA at most when driving the input LEDs at the maximum rated current of 50 mA. While, as we have mentioned above, the current driving or sinking capability is not relevant as far as the steady state is concerned, a large capacitance (in the order of a few mF, as will be discussed in the following) is needed to filter out the large noise produced at the output of the source and therefore the source must be capable of compensating the leakage current through such capacitor and allow reasonable transient times when changing and/or discharging toward a given set point.

Recently, miniaturized solar cells in SOIC packages have been introduced that are capable of output voltages of 4 or 8 V with a maximum short circuit currents of 100 and 50 μA, respectively, under direct sun illumination (CPC18XX series of integrated solar cells by IXYS). By mounting a high intensity LED facing the sensitive surface of the chip it is possible to obtain a programmable floating voltage source. A prototype demonstrating the feasibility of this approach has been built and tested with encouraging results.[16] A few problems still remained, however, for the approach to be considered practical. In the first place, besides the complication of the mechanical arrangement required for coupling the LED acting as controlled light source to the integrated solar cell, the current delivery capability of the cell always remained significantly below 50% of the maximum rated performances. This could be possibly solved by interposing a proper optical system between the LED and the cell, but this would further complicate the design and increase the cost of the system. Moreover, for obtaining reasonable settling time, the cell should be capable of both sourcing and sinking a sufficiently large current to both charge and discharge the filtering capacitor in a short time. A single solar cell can only source current. For obtaining a significant current sinking capability, two cells in anti-parallel combination could be used, one for sourcing and the other one for sinking current. Unfortunately, the integrated solar cell produced by IXYS have an internal single PN junction already connected in anti-parallel with the chain of photodiodes, thus making the anti-parallel connection between two cells not possible. Fortunately enough, however, single packaged LED/solar cell combinations have been recently developed and have become commonplace in the field of power electronic circuits as they can serve as floating drivers for power MOSFETs in switching circuits. There are actually several of such devices being produced by a number of manufacturers, with a number of added options for optimizing the driving of MOSFETs in power circuits. As we are, however, interested in the possibility of using these devices for

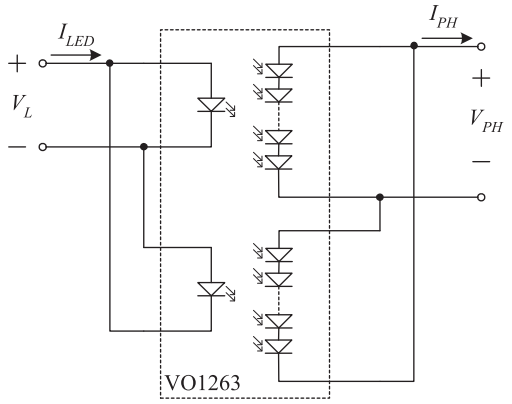

FIG. 2. Connection diagram of the VO1263 device by Vishay Semiconductor for realizing a floating bipolar Current Controlled Current Source (CCCS).

obtaining a low noise programmable voltage source, we selected for our study the VO1263 device by Vishay Semiconductor. Although advertised as a "Dual Photovoltaic MOSFET Driver Solid-State Relay," the VO1263 simply contains two independent optically coupled LED/photodiode array in a compact DIP-8 or SMD-8 packages. The VO1263 can be connected as shown in Fig. 2 for obtaining a bipolar floating voltage source capable of sourcing or sinking currents in excess of 50 μA while providing for an open voltage in excess of $\pm$12 V. By means of a proper combination of two or more VO1263, one can easily increase the output voltage range and/or the current driving capability. The output short circuit current I_{PHSC} of the circuit in Fig. 2 ($I_{PHSC} = I_{PH}$ with $V_{PH} = 0$) is reported in Fig. 3 vs the input LED driving current I_{LED} (the absolute maximum rating for the continuous current in each LED is 50 mA). As it can be noted, good linearity

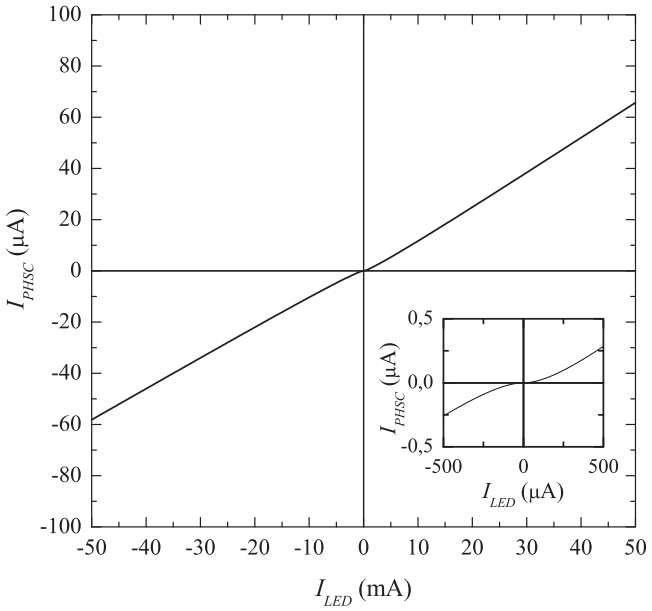

FIG. 3. Short circuit current I_{PHSC} at the output of the circuit in Fig. 2 ($I_{PHSC} = I_{PH}$ when $V_{PH} = 0$) versus the input current driving the LEDs (I_{LED}). A magnified view of the input output characteristic of the CCCS in the region close to the origin is reported in the inset.

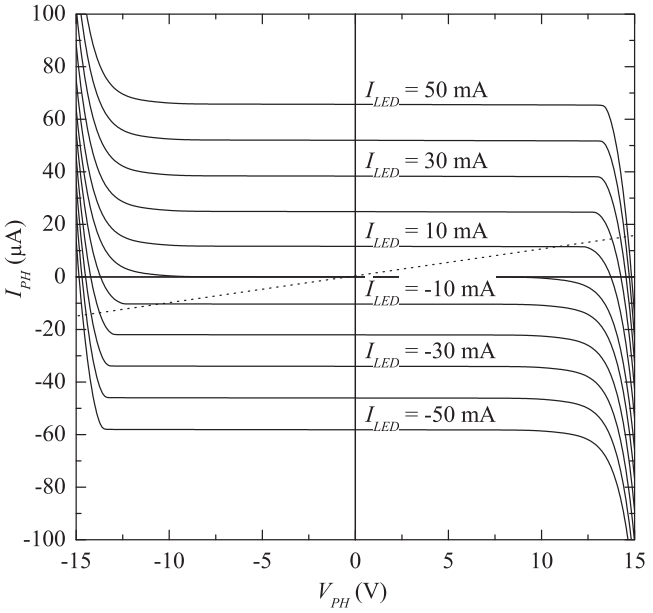

FIG. 4. Output characteristics of the CCCS. The output current I_{PH} is plotted vs the output voltage V_{PH} with the input current driving the LED (I_{LED}) as parameter. The dashed line represents the load curve corresponding to a resistance of 1 MΩ connected to the output port.

is obtained for photo-generated output currents I_{PHSC} above 1 μA and below –1 μA. A difference in the slope of the curve for positive output currents ($I_{PHSC} > 1$ μA, slope $= 1.3 \times 10^{-3}$) and negative output currents ($I_{PHSC} < -1$ μA, slope $= 1.2 \times 10^{-3}$) can be noted that is the overall result of the electrical and optical mismatch between the two LED/photocell array systems in the package. This mismatch is, however, not relevant for our application. The output characteristics of the bipolar floating voltage source are reported in Fig. 4 (note that the reference direction for the current I_{PH} is opposite to what is normally done in reporting the output characteristics of a device, as it is in accordance with what is normally done in discussing the characteristics of a photovoltaic source). It can be easily verified from Fig. 4 that, as it was expected, there is a large region in which the device behaves as a Current Controlled Current Source (CCCS) for output voltages in the range from about -12 V up to 12 V), with the sourced or sunken current essentially coincident with the short circuit current I_{PHSC} for any given value of the LED current. If a resistance R_{PH} is placed in parallel to the output port, the device can be regarded as a current controlled voltage source with the output voltage given by

$$V_{PH} = I_{PH} R_{PH} = \alpha I_{LED} R_{PH}, \tag{3}$$

with α being the ratio I_{PH}/I_{LED} that can be obtained from Fig. 3. Equation (3) applies as long as the operating point stays in the constant output current region in Fig. 4. For instance, the dashed line in Fig. 4 represents the load curve corresponding to $R_{PH} = 1$ MΩ, providing for an output voltage range in excess of $\pm$10 V with a linear dependence of V_{PH} on I_{LED}. Lower values for R_{PH} would result in a larger linear range, while larger values would result in a narrower linear range. As we shall discuss presently, however, the resistance R_{PH} plays an important role as far as the reduction of the

output noise is concerned and, in this respect, it is desirable to select R_{PH} as large as possible, compatibly with the required linear output range.

The floating source described above can only be useful if, in the desired frequency range, the noise level is comparable or lower than the equivalent input noise of the JFET employed in the low noise current source in Fig. 1. As a reference, we will take into consideration the IF3601 by INTERFET that is characterized by an equivalent input noise as low as 10 nV/$\sqrt{}$Hz at 100 mHz, 1 nV/$\sqrt{}$Hz at 1 Hz, and less than 0.5 nV/$\sqrt{}$Hz at frequencies above 10 Hz. This device, in its differential pair version (IF3602), has been used for the design of the ultra-low noise voltage amplifier that will be used for all noise measurements in this work,[17] and therefore we can regard the background noise of this amplifier as the reference noise spectra with respect to which the noise of the source will have to be compared to. As far as the frequency range of interest is concerned, although in some special cases investigations down to 10^{-6} Hz have been reported, experiments seldom extend below 100 mHz.[18,19] The reason why frequencies below 100 mHz are seldom taken into consideration can be easily understood when we observe that for obtaining reliable spectra estimation down to 100 mHz (estimation error below 10%) by using a DFT spectrum analyzer, measurement times in the order of several thousands of seconds may be required.[20] Since the required measurement time is inversely proportional to the lowest frequency of interest, 100 mHz can in fact be regarded as an absolute practical limit for experiments to be carried out in a time scale of a few hours, that is to say within a single day. With these observations in mind, we assumed 100 mHz as the lowest frequency of interest for all experiments in which the programmable source might be employed.

The noise spectra measured at the output of the floating noise source in Fig. 2 with a load resistance $R_{PH} = 1$ MΩ are reported in Fig. 5 for a limited number of output voltages (three uppermost curves). The spectra have been corrected for the load effect of the 3.3 MΩ input resistance of the low noise amplifier used to perform the measurements.[17] However, the spectra are not corrected for the effect of the amplifier input capacitance, whose influence is apparent in the decrease of the measured spectra starting at about 1 kHz. From the analysis of these noise spectra, it is found that, in the low frequency range, the power spectral density S_{IPH} of the current noise generated by the source in Fig. 2 can be modeled as the superposition of a shot noise component due to the sourced DC current I_{PH} ($I_{PH} \approx I_{PHSC}$ in all investigated cases) and a flicker noise component according to the following expression:

$$S_{IPH} = A_f \frac{(I_{PHSC})^\beta}{f} + 2qI_{PHSC}$$
$$A_f \approx 1.5 \times 10^{-6}\ \text{(MKS units)}; \quad \beta \approx 1.64, \tag{4}$$

where q is the elementary charge.

As it can be readily observed from Fig. 5, where the reference spectrum (that is the Background Noise or BN of the preamplifier used for the measurements) is also reported, the voltage noise at the output of the source is, in the worst case, about 60 dB larger than the reference noise. Proper filtering

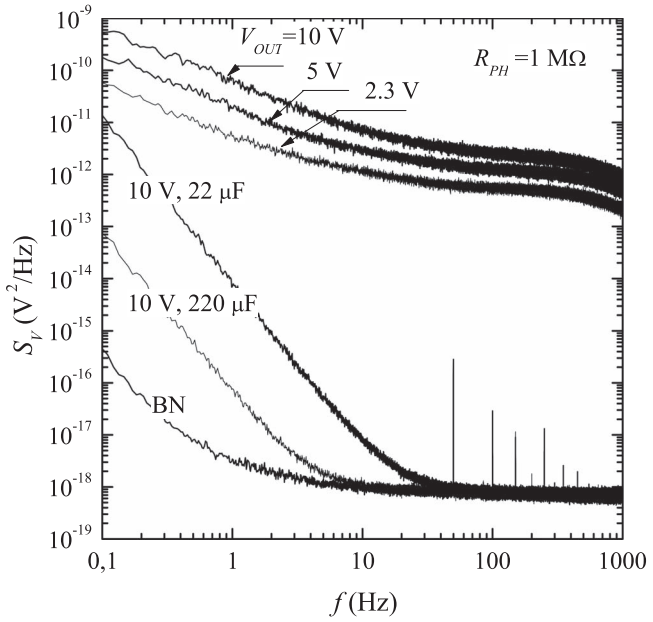

FIG. 5. Voltage noise measurements at the output of the CCCS with a resistance $R_{PH} = 1$ MΩ. All measurements are performed employing an ultra low noise amplifier whose background noise is labeled BN in the figure and are corrected for the loading effect of its input resistance. The three uppermost spectra are measured across R_{PH} with no capacitor in parallel and with I_{LED} adjusted in such a way as to obtain the DC output voltage indicated for each curve. The remaining spectra are obtained when connecting capacitors with different capacitance values in parallel to R_{PH}. When a 10 mF supercapacitor is used, the recorded spectrum coincides with the BN of the amplifier.

down to the minimum frequency of interest (100 mHz) is therefore required. Such a filtering can be obtained by resorting to a capacitor C_{PH} with a sufficiently large capacitance in parallel to the load resistance R_{PH}. Examples of the noise that is obtained at the output of the floating voltage source when connecting a polyester capacitor of 22 μF or 220 μF are reported in Fig. 5. Clearly, even with the largest capacitor (220 μF) we end up with an insufficient attenuation of the noise at frequencies below 10 Hz. It can be easily demonstrated, by taking into account the frequency response of the filter (parallel combination of R_{PH} and C_{PH}) and the shape of the noise spectra, that if the required attenuation (60 dB) is obtained at the minimum frequency of interest, the attenuation will be larger at larger frequencies. An attenuation of 60 dB at 100 mHz can only be obtained if the pole frequency f_{PH} of the $R_{PH}C_{PH}$ combination at the output of the source is 100 μHz or below, since a first order low pass filter introduces an attenuation of 20 dB per decade above the corner frequency. From this observation we have

$$f_{PH} = \frac{1}{2\pi R_{PH} C_{PH}} \le 100\ \mu\text{Hz}$$
$$\Rightarrow (R_{PH} = 1\ \text{M}\Omega) \quad C_{PH} \ge 1.6\ \text{mF}. \tag{5}$$

Until a few years ago, realizing such high capacitance values for applications in the field of low frequency noise measurements was a quite challenging task. Conventional electrolytic capacitors are not suitable for this purpose because of micro-discharge effects through the dielectric layer that occur at voltages well below the maximum rated voltages, resulting

in additional noise components at very low frequencies. On the other hand, high voltage (≥100 V) polypropylene or polyester film capacitor that do not suffer from such instabilities are available with capacitances up to a few tens of microfarads and reaching capacitances above 1 mF could only be obtained by a bulky (and expensive) combination of several tens of such capacitors. Fortunately enough, the relatively recent introduction of supercapacitors (or ultracapacitors) does offer the possibility of obtaining high capacitances in a very compact size. In a way, when resorting to supercapacitors, the problem we face is opposite to the one we face in the case of plastic dielectric capacitors, since supercapacitors are normally available with capacitances much larger than those required according to Eq. (5). While from the point of view of noise attenuation the larger the capacitance the better, there are other aspects that advice to select the minimum capacitance satisfying Eq. (5). Indeed, because of the limitation in the maximum current that can be sourced by the floating source (about 60 μA), the time required for charging or discharging the capacitor up to the desired value is directly proportional to its capacitance. Furthermore, supercapacitors suffer from relatively large residual leakage currents whose value increase as the capacitance increases. Therefore, for our application we searched for the supercapacitor with the minimum capacitance that was available on the market with a rated voltage above the targeted maximum voltage of 10 V. We selected the BestCap 10 mF supercapacitor produced by AVR with a rated voltage of 12 V and a compact size of about 20 mm × 15 mm × 6 mm. When this capacitor is used in parallel to R_{PH}, with the LED driving current adjusted in such a way as to obtain a 10 V output, the measured output noise spectrum coincides with the background noise of the amplifier, demonstrating that, down to 100 mHz, the noise generated by the floating source is much lower than the reference noise.

The complete circuit required for obtaining a very low noise, high accuracy programmable current source is discussed in Sec. II.

II. PROGRAMMABLE LOW NOISE CURRENT SOURCE

The complete schematic of the low noise, high accuracy programmable current source is reported in Fig. 6. The circuit reduces to the circuit in Fig. 1 where the battery V_B is replaced by the low noise floating current source and a feed-back loop is added for setting the value of the desired current starting from the output of the AD667 high accuracy DA converter. Instead of employing a single very low noise IF3601 JFET for J_1, we made the choice of employing four 2SK170 low noise JFETs in parallel. In terms of equivalent input voltage noise, the two configurations are almost equivalent for supplied currents in the mA range. When paralleling JFETs, one must be careful in selecting devices with quite similar actual parameters for the total current to be uniformly divided among all the devices. This pre-selection burden is counterbalanced by the fact that devices such as the 2SK170 are quite cheap and easily available on the market, while the IF3601, which is undoubtedly characterized by excellent performances, is much more expensive and less easily found as part of the catalogues of the most common electron device resellers.

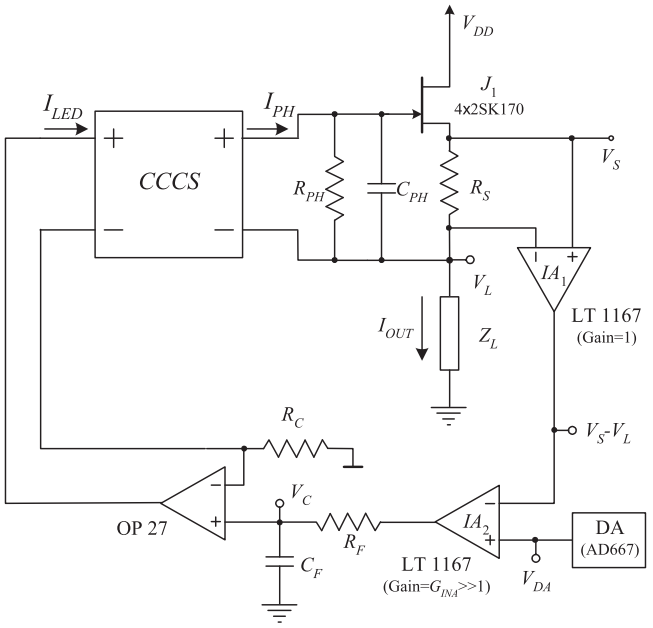

FIG. 6. Simplified schematic of the complete programmable low noise current source. The block CCCS is the circuit in Fig. 2, DA is a high accuracy 12 bit DA converter (AD667 by Analog Devices), J_1 is obtained as the parallel combination of four matched 2SK170 JFETs. The system supply is ±12 V obtained by resorting to lead acid batteries.

The current to be supplied is set as the result of the value of the resistance R_S and of the voltage at the output of the DA converter AD 667. If the gain G_{INA} of the instrumentation amplifier, IA_2, that acts as error amplifier, is sufficiently large, at steady state we have

$$(V_S - V_L) = R_S I_{OUT} \approx V_{DA} \rightarrow I_{OUT} \approx \frac{V_{DA}}{R_S}. \qquad (6)$$

The output of IA_2 supplies the input of a transconductance amplifier (after a low pass filter whose role will be presently discussed) that drives the LEDs of the CCCS in order to bring the bias at the gate of the JFET to the correct value for obtaining the desired output current. The resistance R_C is an excess free resistance whose value is chosen in such a way as to allow to reach, during transients, the maximum rated current of 50 mA through the LEDs so that charging/discharging times can be reduced to a minimum. With the system supplied with ±12 V lead batteries, the maximum voltage swing at the output of IA_2 is about ±10 V, thus setting the value of R_C to 200 Ω. While the feedback configuration in Fig. 6 can certainly allow to obtain good accuracy in setting the value of the supplied current, the most important issue to be addressed is the level of additional noise that is introduced by the feedback loop. There are several sources of noise that can dramatically degrade the noise performances of the current source and, indeed, the most challenging task in the design we propose has been to couple good performances in terms of accuracy to excellent performances in terms of output noise.

One of the most critical component in Fig. 6 is the instrumentation amplifier IA_1 that has to be used for reading the voltage across the resistance R_S for producing an equal voltage (referenced to ground) at the output to be compared with the reference voltage V_{DA}. The input bias current as well as

the current noise at the input connected to the node V_L flow entirely through the load, thus adding a DC current offset and, more importantly, a contribution to the system output current noise. It is for this reason that we have selected the very low input bias current and very low input current noise instrumentation amplifier LT1167 by Linear Technology. For supplied currents to the load in the order from a few μA to a few mA, the input bias current of the LT1167 (80 pA typ.) can be considered negligible while its input current noise at the lowest frequency of interest (100 mHz) is in the order of 1 pA/$\sqrt{\text{Hz}}$. Note that, with a supplied current in the order of a few mA, the equivalent input voltage noise of J_1 at 100 mHz is in the order of 25 nV/$\sqrt{\text{Hz}}$ that, with $R_S = 1$ kΩ, translates in a current noise to the load in the order of 25 pA/$\sqrt{\text{Hz}}$. In these conditions, from IA_1 can be considered negligible. Lower input current noise amplifiers could be used; however, this would result in larger equivalent input noise voltages that, as we shall presently discuss, must be maintained as low as possible as well. With the exception of the equivalent input current noise at the non-inverting input of the OP27 in Fig. 6, it can be easily shown that all other sources of current noise in the circuit have a negligible effect at all frequencies of interest. If the value of C_F is sufficiently large (in the order of a few mF), also the equivalent input current of the OP27 can be neglected with respect to the effect of its equivalent input voltage noise.[6] Therefore, assuming C_F to be a 10 mF supercapacitor (that is identical to C_{PH}), we are left with the problem of evaluating the effect on the load of all the equivalent voltage noise sources in the control loop. In order to simplify the determination of all these contributions to the output current noise we will make the following assumptions:

- As far as the calculation of the noise contribution from the control loop is concerned, we will assume the JFET, the resistance R_S, the *CCCS* and the resistance R_{PH} as noiseless devices.
- As long as the impedance Z_L is small compared to the output impedance of the current source, we can replace it with a short circuit.

With these assumptions, we may refer to the simplified schematic in Fig. 7 for noise calculations. Note that the first instrumentation amplifier (IA_1) is not present in the figure because of its unitary gain; however, its noise contribution is accounted for by means of the noise source e_{nIA1} whose equivalent spectral density is equal to that of the equivalent input voltage noise source of IA_1. This source is in series with the equivalent input voltage noise source of IA_2 and since, as can be verified in the data-sheet from the manufacturer, the PSD of e_{nIA2} for a gain much larger than one ($G_{INA} \ll 1$) is much smaller than the PSD of e_{nIA1}, relative to the same instrumentation amplifier with a unitary gain, we can neglect the contribution by e_{nIA2}. The transfer function from each noise source to the node V_S can be quite easily calculated using the following relationships:

$$V_C = [(e_{nDA} - e_{nIA1} - V_S)G_{INA} + e_{nRF}] \times \frac{1}{1 + s\tau_F} \quad \tau_F = R_F C_F,$$

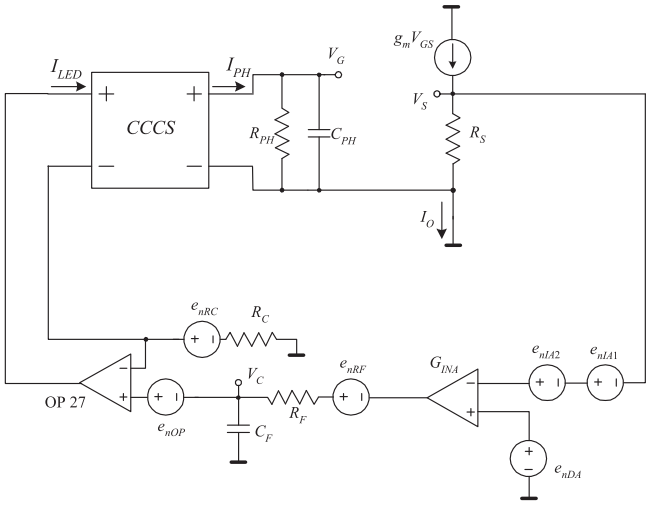

FIG. 7. Simplified small signal equivalent circuit for the calculation of the noise introduced by the control circuit.

$$I_{LED} = (V_C + e_{nOP} - e_{nRC}) \times \frac{1}{R_C},$$
$$I_{PH} = \alpha I_{LED},$$
$$V_G = I_{PH} \times \frac{R_{PH}}{1 + s\tau_{PH}} \quad \tau_{PH} = R_{PH} C_{PH},$$
$$V_S = V_G \frac{g_m R_S}{1 + g_m R_S} \approx V_G \quad g_m R_S \gg 1. \tag{7}$$

We obtain, for V_S:

$$V_S = H(s)\left\{e_{nDA} - e_{nIA1} + \frac{1}{G_{INA}}[e_{nRF} + (e_{nOP} - e_{nRC})(1 + s\tau_F)]\right\},$$
$$H(s) = \frac{T(s)}{1 + T(s)}, \tag{8}$$
$$T(s) = \frac{T_0}{(1 + s\tau_F)(1 + s\tau_{PH})} \quad T_0 = \frac{\alpha R_{PH}}{R_C} G_{INA}.$$

And, in terms of power spectral densities, with all noise sources uncorrelated, we have

$$S_{VS} = |H(j\omega)|^2 \left\{S_{enDA} + S_{enIA1} + \frac{1}{G_{INA}^2}[S_{enRF} + (S_{enOP} + S_{enRC})|1 + j\omega\tau_F|^2]\right\}. \tag{9}$$

Once we know S_{VS}, S_{IOUT} can be simply calculated as $S_{VS}/(R_S)^2$.

The most important contribution to the noise at node V_S at very low frequencies comes from the noise at the output of the DA converter. Such a noise level can exceed 10^{-11} V^2/Hz (3.3 μV/$\sqrt{\text{Hz}}$) at 100 mHz.[12] For comparison, the power spectrum of the equivalent input voltage noise source S_{enIA1} of the LT1167 with gain = 1 at the same frequency is ten times

smaller. As far as the other terms are concerned, their relative weight can only be estimated after dimensioning the circuit parameters G_{INA}, R_F and C_F. We can, however, anticipate, in order to simplify the discussion, that for obtaining high DC accuracy, G_{INA} will have to be in the order of 100, that the resistance R_F will be in the order of 10 kΩ and that the pole frequency f_F will be in the order of 1 mHz. Therefore, with reference to Eq. (9), the contribution in the curly brackets from R_F is clearly negligible at all frequencies as it would correspond to the thermal noise of a 1 Ω resistor (4×10^{-21} V^2/Hz). Moreover, with $R_C = 200$ Ω ($S_{enRC} = 8.3 \times 10^{-19}$ V^2/Hz), it is the equivalent input noise of the OP27 that dominates in the sum $S_{enOP} + S_{enRC}$ (S_{enOP} is 2.5×10^{-16} V^2/Hz at 100 mHz and about 9×10^{-18} V^2/Hz at frequencies larger than a few Hz). With $f_F = 1$ mHz and $G_{INA} = 100$, and taking into account the $1/f$ behavior of the noise at the output of the DA converter, it can be easily verified that the contribution of S_{enOP} is negligible with respect to S_{enDA} up to about 10 Hz. Note that, as we shall presently discuss, the increase in noise due to the term $j\omega\tau_F$ is only apparent when we take into account the behavior of the frequency response $H(j\omega)$.

With such a high noise contribution coming from the DA converter, it is clear that while we need T_0 to be large for reaching good DC accuracy ($|H(j0)| \approx 1$), we also need $|T|$ to be sufficiently small at all frequencies of interest to filter out the DA noise contribution. This is the main reason why we need to introduce a second pole at $f_F = 1/(2\pi\tau_F) \ll 100$ mHz in order to obtain the required attenuation of the noise coming from the control circuit, since the single pole at $f_{PH} = 1/(2\pi\tau_{PH})$ would not be sufficient to obtain, at the same time, high accuracy, DA noise reduction and acceptable response time upon current setting change. If we restrict our attention to frequencies larger than $f_{MIN} = 100$ mHz, assuming both f_{PH} and f_F to be much smaller than f_{MIN}, we have

$$T(j2\pi f) \approx -\frac{f_F f_{PH} T_0}{f^2} \quad f \gg f_{MIN}. \tag{10}$$

Note, moreover, that if we assume that at all frequencies of interest ($f > f_{MIN}$) $|T| \ll 1$, we have

$$|H(j\omega)| = \left|\frac{T(j2\pi f)}{1 + T(j2\pi f)}\right| \approx |T(j2\pi f)| \approx \frac{f_F f_{PH} T_0}{f^2}. \tag{11}$$

In order to reduce the noise introduced by the DA down to a level comparable to the equivalent input noise source of J_1 at the lowest frequency of interest we need an attenuation in the order of at least 50 dB, that is

$$|T(j2\pi f_{MIN})|^2 < 10^{-5} \Rightarrow \frac{f_F f_{PH} T_0}{f_{MIN}^2} < \sqrt{10^{-5}}$$
$$\Rightarrow f_F G_{INA} < \frac{\sqrt{10^{-5}} f_{MIN}^2 R_C}{\alpha R_{PH} f_{PH}}. \tag{12}$$

Note that if the desired attenuation is obtained at the lowest frequency of interest, a much higher attenuation will be obtained at higher frequencies because of the dependency of T on the frequency ($|T|$ decreases by 80 dB/decade). The rightmost inequality in Eq. (12) has been rearranged in order to stress the fact that a constraint exists on the value of G_{INA} (that essentially sets the DC accuracy) and the pole frequency of the filter at the output of the error amplifier in order not to add excess noise to the load.

When we use the values of the parameters according to what previously discussed, we have

$$f_F G_{INA} < \frac{\sqrt{10^{-5}} f_{MIN}^2 R_C}{\alpha R_{PH} f_{PH}} \approx 0.3 \text{ Hz}. \tag{13}$$

At the same time, with the given values of α, R_C, and R_{PH}, we have

$$T_0 = \frac{\alpha R_{PH}}{R_C} G_{INA} \approx 6.5\, G_{INA}. \tag{14}$$

This means that, in order to obtain an accuracy better than 1% in setting the DC output current, we require G_{INA} to be in the order of 100 and, therefore, f_F in the order of 1 mHz. As the value of C_F has to be 10 mF for insuring a negligible noise contribution from the equivalent input current source at the non inverting input of the OP27, with $R_F = 10$ kΩ we obtain $f_F \approx 1.6$ mHz thus satisfying all the requirements for obtaining high accuracy and no excess noise to the output current coming from the control circuit.

If we require larger accuracy, we may increase G_{INA} and correspondingly increase R_F in order to satisfy Eq. (13). However, it must be noted that the choice of G_{INA} and f_F has an effect on the transient response of the system upon changing the DA setting. Indeed, as it is obvious from Fig. 7, the transfer function from the DA output toward the output V_S is the same that has been calculated for the noise source e_{nDA}. We have, therefore,

$$\frac{V_S}{V_{DA}} = H(s). \tag{15}$$

It is quite easy to show that $H(s)$ can be written in the form

$$H(s) = \frac{T_0}{1 + T_0} \times \frac{1}{\frac{\tau_F \tau_{PH}}{1+T_0} s^2 + s\frac{\tau_F + \tau_{PH}}{1+T_0} + 1}, \tag{16}$$

and, assuming $T_0 \gg 1$, $\tau_{PH} \gg \tau_F$,

$$H(s) \approx \frac{1}{\frac{\tau_F \tau_{PH}}{T_0} s^2 + s\frac{\tau_{PH}}{T_0} + 1} = \frac{1}{\frac{s^2}{\omega_0^2} + \frac{s}{Q\omega_0} + 1},$$
$$\omega_0 = \sqrt{\frac{T_0}{\tau_{PH}\tau_F}} = 2\pi\sqrt{\frac{f_{PH}\alpha R_{PH}}{R_C} f_F G_{INA}}, \tag{17}$$
$$Q = \sqrt{\frac{f_{PH}\alpha R_{PH}}{R_C} \times \frac{G_{INA}}{f_F}}.$$

With the values for the parameters used before ($G_{INA} = 100$, $f_{PH} = 16$ μHz) we have $\omega_0 = 25 \times 10^{-3}$ rad/s (corresponding to a frequency $f_0 = 4$ mHz) and $Q = 2.55$, that is we obtain a moderate overshoot in response to an input step (assuming the system to remain in linearity). If we require a larger DC accuracy (larger G_{INA}), according to Eq. (13) we must proportionally decrease f_F, and this, assuming the product $G_{INA} f_F$ to remain the same, would correspond to the same value of f_0

but a larger value of Q, thus inducing larger oscillations during the transient and, hence, larger settling time.

It is for this reason that, in the prototype we have built and tested, G_{INA} was limited to 100, thus achieving a reasonable compromise between settling time and accuracy. Note that, because of the large gain in the feedback loop, upon DA voltage changes in the order of a few hundreds mV, the output of IA_2 is likely to be in saturation during most of the transient and linearity is regained when the voltage across R_S is within less than 100 mV of the final DC steady state value. In these conditions, upon turn on and setting a DA output voltage of a few volts, steady state is reached in a few tens of minutes (typically less than half an hour) that, when willing to accurately estimate power spectra down to 100 mHz, is a quite reasonable time.

III. EXPERIMENTAL RESULTS

A prototype of the circuit in Fig. 6 has been built and tested. The gain of IA_2 was set to 100 and the resistance R_S was set to 1 kΩ as discussed in the previous paragraph.

As a first test, the node V_L was shorted to ground and the voltage noise at the output V_S was measured. The background noise of the ultra low noise voltage preamplifier used for all measurements is reported in Fig. 8 (ULNA BN). The noise measured at the output V_S when $Z_L = 0$ (V_L shorted to ground) for a DA setting of 4 V (corresponding to a current $I_{OUT} = 4$ mA) is also reported in Fig. 8. As it can be noted, at very low frequencies the measured noise essentially coincides with the BN of the amplifier, so that we can only conclude that the noise at V_S, that we expect to coincide with the equivalent input voltage noise of J_1, thanks to the parallel combination of four 2SK170, is comparable or even lower than the equivalent input voltage noise of the ultra low noise preamplifier used for the measurements. At higher frequencies, a clear indication of an additional noise component can be observed that can be attributed to the thermal noise from R_S (the noise contribution from R_S is attenuated by the low JFET equivalent output impedance at the node V_S).

In a second set of measurements we employed excess noise free resistors for the load Z_L and we measured the voltage noise at the output V_L. The expected power spectrum can be written as

$$S_{VL}(f) = S_{IOUT} R_L^2 + 4kTR_L \approx (S_j + 4kTR_S)\left(\frac{R_L}{R_S}\right)^2 + 4kTR_L, \quad (18)$$

where R_L is the resistance employed as a test load. In order to allow the estimation of S_{IOUT} from Eq. (18), two conditions must be met: (a) the noise S_{VL} should be much larger than the BN of the voltage amplifier used for the measurement and (b) the noise due to the current source must be large enough to allow the subtraction of the thermal noise contribution from the resistor used as a test load. Both these conditions can be obtained with a sufficiently large value of R_L with respect to R_S. At the same time, however, large values for R_L limit the maximum value of the current that can be delivered to the load with the JFET in the active region since:

$$V_S = (R_S + R_L) I_{OUT}. \quad (19)$$

With $R_L = 3.3$ kΩ we obtain a reasonable compromise between the need of maintaining a high value for S_{VL} (S_j is multiplied by a factor 10) and allowing to set currents in the mA range (up to about 2 mA). The measured spectrum when I_{OUT} is set to 1.8 mA is indeed sufficiently large (Fig. 8) for the BN of the amplifier to be neglected at all frequencies. In these conditions, Eq. (18) can be used for estimating the spectrum S_{IOUT}. The spectrum S_{IOUT} is reported in Fig. 9 confirming that the current noise at the output of the source reduces to that introduced by the JFET and the resistance R_S as was expected by our design. In particular, when delivering an output current of 1.8 mA, we obtain a current noise of just 6×10^{-22} A^2/Hz (or 25 pA/$\sqrt{}$Hz) at 100 mHz and less than 3×10^{-23} A^2/Hz (or 6 pA/$\sqrt{}$Hz) for $f > 1$ Hz. By integrating the power spectrum between 0.1 and 10 Hz we can estimate the RMS noise in such a bandwidth to be about 13 pA. As a comparison, the RMS noise in the same bandwidth and for the

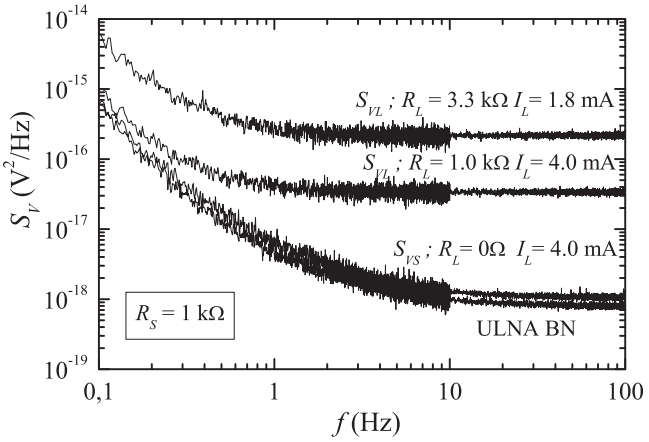

FIG. 8. Voltage noise spectra measured on the prototype. ULNA BN is the background noise of the amplifier. S_{VS} is the spectrum of the voltage noise at node V_S with node V_L grounded ($R_L = 0$). S_{VL} are the spectra of the noise voltage across the load (R_L) in different operating conditions.

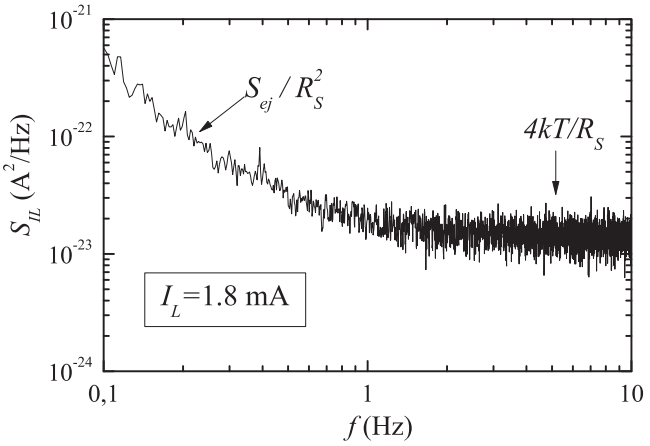

FIG. 9. Power spectrum of the current fluctuations across a load of 3.3 kΩ when I_{OUT} is set to 1.8 mA. The current spectrum is obtained from the voltage spectrum S_{VL} obtained with $R_L = 3.3$ kΩ, $I_L = 1.8$ mA (reported in Fig. 8) by using Eq. (18).

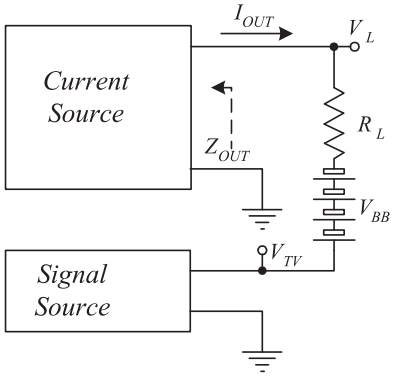

FIG. 10. Measurement configuration for the estimation of the output impedance of the current source. The voltage V_{BB} is 40 V (obtained by connecting several batteries in series) so that the DC voltage V_L is close to 0 when $I_{out} = 2$ mA with $R_L = 20$ kΩ.

same supplied current of the Keithley model 6220 precision current source (advertised as characterized by exceptionally low current noise) is in the order of 40 nA, that is more than 60 dB larger than what is obtained in our prototype. Note that, as we have noted before, the resistance R_S plays an important role in setting the output noise. Increasing the value of R_S for the same output current may allow to obtain less noise at the cost of a smaller maximum allowed voltage drop across the load.

A final test is reported with the load resistance R_L set to 1 kΩ so that a current of 4 mA can be made to flow through the load (Fig. 8). Also in this case the measured spectrum is very close to the one expected from Eq. (18) save at very low frequencies ($f < 500$ mHz) where the contribution of the BN of the amplifier is no longer negligible. As far as accuracy is concerned, the residual error at the input of IA_2 resulted well below 1% in all experiments (close to 0.3% in all cases).

As we have mentioned in the Introduction, a relevant parameter for a current source is its output impedance. The data sheet for the 2SK170 do not include sufficient details about the drain to source parasitic resistance in the active region for allowing a reliable estimation of this parameter, and therefore we made an attempt for a direct measurement of the equivalent output impedance of the system with the approach reported in Fig. 10. The series of batteries V_{BB} together with a high resistance load ($R_L = 20$ kΩ) is used for maintaining the system in linearity when delivering about 2 mA with $R_S = 1$ kΩ. With $V_{BB} = 40$ V, the DC voltage at node V_L is close to 0. A programmable signal generator provides for a sinusoidal test voltage V_{TV} with a peak to peak amplitude V_{PPTV} of 300 mV at any desired frequency while the amplitude of the AC voltage at node V_L is monitored by means of a digital oscilloscope. Note that, since we are interested in frequencies well below 1 Hz, the oscilloscope input has to be DC coupled to node V_L. The signal at the node V_L was recorded with the vertical scale of the oscilloscope set to 100 mV/div resulting in a voltage resolution ΔV of about 3 mV (±400 mV range with a resolution of 8 bit). The acquisition was synchronized with the signal generator in order to allow averaging for reducing the error in the estimation of the signal amplitude. In these conditions, the peak to peak amplitude V_{PPVL} of the AC signal at node V_L can provide an estimate of the equivalent output impedance $|Z_{OUT}|$ starting from:

$$V_{PPVL} = V_{PPTV} \frac{|Z_{OUT}|}{|Z_{OUT} + R_L|}. \quad (20)$$

In the above mentioned conditions, V_{PPVL} was found to be smaller than V_{PPTV} by an amount of less than 3 ΔV (repeated measurements of the difference between V_{PPTV} and V_{PPVL} resulted in values from 0 to 3 ΔV due to quantization). Because the observed difference is quite close to the resolution limit of the measurement system, we were not able to accurately extract the output impedance. However, assuming the worst case (3 ΔV), from Eq. (20) we can estimate the output impedance to be larger than 1 MΩ at all investigated frequencies from 100 mHz up to 1 kHz.

IV. CONCLUSIONS

We have demonstrated that by using a programmable floating voltage source and a proper control feedback it is possible to design programmable current sources characterized by high accuracy, very low noise at low frequencies and high output impedance. The accuracy in setting the desired DC current is better than 1%; however, better accuracies can be obtained if one is willing to accept higher levels of noise at very low frequencies. In the prototype that we have designed and built we obtain, for sourced currents in the mA range an RMS noise level in the bandwidth from 0.1 to 10 Hz that is orders of magnitude below that of commercially available instrumentation. While using batteries with a proper series resistance for setting the current through a device under test remains the approach that can provide for the lowest possible level of background noise at low frequencies, the performances of the current source we propose are to be regarded as excellent especially since they are obtained together with programmability and high accuracy in setting the DC value of the supplied current. The fact that the system is quite compact with respect to other solutions proposed in the literature, has to be regarded as a significant feature in itself, since it simplify the integration of the programmable current source as part of completely automated noise measurement systems.

ACKNOWLEDGMENTS

This work has been funded by MIUR by means of the national Program PON R&C 2007–2013, project "Elettronica su Plastica per Sistemi Smart-disposable" (PON02_00355_3416798).

[1]L. K. J. Vandamme, IEEE Trans. Electron Devices **41**, 2176 (1994).
[2]C. Ciofi, G. Giusi, G. Scandurra, and B. Neri, Fluctuations Noise Lett. **4**, L385 (2004).
[3]R. J. W. Jonker, J. Briaire, and L. K. J. Vandamme, IEEE Trans. Instrum. Meas. **48**, 730 (1999).
[4]S. Linzen, T. L. Robertson, T. Hime, B. L. T. Plourde, P. A. Reichardt, and J. Clarke, Rev. Sci. Instrum. **75**, 2541 (2004).
[5]C. Ciofi, M. De Marinis, and B. Neri, Mircoelectron. Reliab. **36**, 1851 (1996).
[6]C. Ciofi, F. Crupi, C. Pace, and G. Scandurra, IEEE Trans. Instrum. Meas. **52**, 1533 (2003).

[7]L. T. Harrison, *Current Sources and Voltage References* (Elsevier, Oxford, 2005), p.137.
[8]C. D. Motchenbacher and J. A. Connelly, *Low-Noise Electronic System Design* (John Wiley and Sons Inc., New York, 1993).
[9]C. Ciofi, R. Giannetti, V. Dattilo, and B. Neri, IEEE Trans. Instrum. Meas. **47**, 78 (1998).
[10]D. Talukdar, R. K. Chakraborty, S. Bose, and K. K. Bardhan, Rev. Sci. Instrum. **82**, 013906 (2011).
[11]C. Pace, C. Ciofi, and F. Crupi, IEEE Trans. Instrum. Meas. **52**, 1251 (2003).
[12]G. Scandurra, G. Giusi, and C. Ciofi, Rev. Sci. Instrum. **85**, 044702 (2014).
[13]G. Scandurra and C. Ciofi, in *Prooceedings of the 21th International Conference on Noise and Fluctuations (ICNF)*, Toronto, Canada, 12–16 June 2011.
[14]E. M. Spinelli and M. A. Mayosky, IEEE Trans. Biomed. Eng. **47**, 1616 (2000).
[15]G. Scandurra, G. Cannatà, and C. Ciofi, IEEE Trans. Instrum. Meas. **62**, 1107 (2013).
[16]G. Scandurra, G. Cannatà, and C. Ciofi, in *Prooceedings of the 22nd International Conference on Noise and Fluctuations (ICNF)*, Montpellier, France, 24–28 June 2013.
[17]G. Cannatà, G. Scandurra, and C. Ciofi, Rev. Sci. Instrum. **80**, 114702 (2009).
[18]F. N. Hooge, T. G. M. Kleinpenning, and L. K. J. Vandamme, Rep. Prog. Phys. **44**, 479 (1981).
[19]I. R. M. Mansour, R. J. Hawkins, and G. G. Bloodworth, Radio Electron. Eng. **35**, 212 (1968).
[20]G. Giusi, G. Scandurra, and C. Ciofi, Fluctuations Noise Lett. **12**, 1350007 (2013).